

# Texel-Based Prototypes of Regular Mosaics

Georgy Gimel'farb\*

*CITR, Department of Computer Science  
Tamaki Campus, University of Auckland  
Private Bag 92019, Auckland 1  
g.gimelfarb@auckland.ac.nz*

## Abstract

*We consider a special case of spatially homogeneous textures such as regular mosaics that can be described as tilings where each tile represents the same rectangular texel. The orientation and size of the texel are estimated from the model-based interaction map (MBIM) describing multiple pairwise pixel interactions in a given training sample. The MBIM is obtained using the Gibbs random field model of the texture. Large-size prototypes of such textures can be formed fast by estimating and replicating the texel.*

## 1 Introduction

Basic feature of a texture is spatial self-similarity, that is, similarity of certain pixel neighbourhoods acting as local prototypes. Such characteristic neighbourhoods are usually called texels [6]. A texture is formed by their spatial replication under specific deterministic or stochastic rules of mutual placement. Each replica may have geometric and photometric deviations from the texel that do not effect the similarity. Generally, a rich variety of possibilities exist for choosing texels, rules of their arrangement, and ranges of admissible deviations in each texture.

The ambiguity is reduced if only translation invariant textures formed by replicating a single texel are considered. At lower levels of generalisation such texel may contain own fine repetitive details with not only translational but also rotational, scale, or other types of similarity. But we restrict our consideration to a limited number of translation invariant natural textures that can be formally described by only a single texel. For practical purposes, this problem appears worthy of investigation because the texel-based description holds considerable promise for fast realistic simulation of these textures.

Recently a notable advance has been made in texture simulation by choosing signals (gray levels or colours) in

each pixel so that its particular neighbourhood approximates the similar pixel neighbourhoods of a given training sample [2–5, 7, 9–11]. The neighbourhood retains the deterministic spatial structure of signal interactions in the training sample. The approximation extrapolates the training structure to a simulated image of other size and yields random deviations from the training signals.

In most cases the characteristic neighbourhoods are involved implicitly through spatial features of a multi-resolution image representation such as relative frequencies of top-to-down signal co-occurrences along a Laplacian or steerable wavelet image pyramid [2, 10]. A simulated pyramid replicates, up to a certain similarity threshold, the corresponding top-to-down chains of the training signals.

A non-parametric Markov random field model of multi-resolution textures in [9] describes a heuristically chosen small close-range pixel neighbourhood (e.g. the squares  $7 \times 7$ ) by conditional relative frequency distributions of all the multi-resolution signals in such a neighbourhood. Assuming that the neighbourhoods are statistically independent, the distributions are roughly estimated from the training signals using clustering techniques. Texture simulation approximates the training distributions with the simulated ones using a constrained multi-resolution optimisation.

In the case of a single-resolution texture, Gibbs random field models with multiple pairwise pixel interactions [4, 5, 11] involve a translation invariant pixel neighbourhood that can be explicitly estimated for each particular texture from the training sample. This discontinuous “star-like” radially symmetric neighbourhood consists of the most characteristic near and distant pixels independently interacting with the central one. The simulation performed by stochastic approximation based on stochastic relaxation approximates the training frequency distributions of signal co-occurrences in the characteristic pixel pairs by the corresponding distributions for the simulated texture.

A non-parametric texture sampling [3] uses a heuristically chosen square around each pixel as an explicit structure-preserving neighbourhood. To simulate a texture, a small seed is taken randomly from the training sample and then extended in a pixelwise mode to a desired size. Each

---

\*This work was partially supported by the University of Auckland Research Committee grants 9343/3414113 and 9393/3600529 and the Marsden Fund research grant UOA122.

new pixel is added by an equiprobable choice from among the already obtained pixels with closely similar neighbourhoods. Generally such pixelwise extrapolation accumulates local errors rupturing the desired texture. The patch-based non-parametric sampling in [7] tries to avoid the degradation by adding at each step not a single pixel but a small rectangular patch of the empirically chosen size. The patch is equiprobably chosen from among the already obtained patches with the similar neighbourhoods.

All the above techniques are efficient in simulating different stochastic and regular natural textures. But most of them are impracticable for simulating large-size images because of excessively large volumes of computations per pixel. The patch-based non-parametric sampling [7] is much faster than other approaches but the quality of simulation depends on how adequate is the empirically chosen patch.

This paper investigates possibilities of fast simulation of large-size prototypes of certain regular mosaics by quantitative estimation and replication of their texels. The estimation is based on the above-mentioned Gibbs random field model that explicitly describes the spatial structure of multiple pairwise pixel interactions in the training sample.

## 2 Gibbs texture model

Let  $\mathbf{R}$  and  $\mathbf{Q}$  denote an arithmetic lattice and a finite set of image signals, respectively. Let  $g : \mathbf{R} \rightarrow \mathbf{Q}$  be a digital image. The Gibbs random field model of a spatially homogeneous texture accounting for only pairwise pixel interactions is given by the Gibbs probability distribution

$$\Pr(g|\mathbf{A}, \mathbf{V}) \propto \exp \left( \sum_{a \in \mathbf{A}} E_a(g|V_a) \right) \quad (1)$$

where the set  $\mathbf{A}$  indicates a characteristic translation invariant neighbourhood  $\{(i+a) : a \in \mathbf{A}\}$  of each pixel  $i \in \mathbf{R}$  and  $E_a(g|V_a)$  is a partial energy of pairwise pixel interactions in a family  $\mathbf{C}_a = \{(i, i+a) : i, i+a \in \mathbf{R}\}$  of translation invariant pixel pairs, or cliques of the neighbourhood graph, separated in the lattice by the same relative inter-pixel shift  $a$ :

$$E_a(g|V_a) = \sum_{(i, i+a) \in \mathbf{C}_a} V_a(g_i, g_{i+a})$$

Pixel interactions in the clique families are quantitatively given by a bounded potential  $\mathbf{V} = \{V_a : a \in \mathbf{A}\}$  where  $V_a : \mathbf{Q} \times \mathbf{Q} \rightarrow \mathcal{R} = (-\infty, \infty)$  is a potential function for the clique family  $\mathbf{C}_a$ . The neighbourhood  $\mathbf{A}$  defines the geometric structure of translation invariant pairwise pixel interactions in terms of the most distinctive interacting pixel pairs  $(i, i+a)$ .

As shown in [4], the first approximation of the maximum likelihood estimate of the potential  $V_a = \{V_a(q, s) : q, s \in$

$\mathbf{Q}\}$  for a given training sample  $\hat{g}$  is proportional to the centred relative frequency distribution  $F_a(\hat{g}) = \{F_a(q, s|\hat{g}) : q, s \in \mathbf{Q}\}$  of the signal co-occurrences  $(\hat{g}_i = q, \hat{g}_{i+a} = s)$  in the cliques of the family  $\mathbf{C}_a$ . Thus the approximate partial energy of pixel interactions is:

$$E_{a,0}(\hat{g}) = \sum_{(q,s) \in \mathbf{Q}^2} F_a(q, s|\hat{g}) \left( F_a(q, s|\hat{g}) - \frac{1}{|\mathbf{Q}|^2} \right) \quad (2)$$

and the clique families specified by a large search set  $\mathbf{W}$  of the inter-pixel shifts  $a$  can be ranked by their interaction energies as well as the characteristic interaction structure  $\mathbf{A}$  can be estimated by selecting the top-rank partial energies [4, 5, 11].

Figures 1 and 2 show training samples  $128 \times 128$  of the natural image textures D1, D6, D14, D20, D21, D34, D53, D55, D65, and D101 from [1] and Fabric0008, Tile0007, and Textile0025 from [8]. Each sample is accompanied with the scaled image  $81 \times 81$  of the model-based interaction map (MBIM)  $\mathbf{E}(\hat{g}) = \{E_{a,0}(\hat{g}) : a \in \mathbf{W}\}$  showing the deterministic structure of translation invariant pairwise pixel interactions. Every spatial position  $a \equiv (x, y)$  of the image of the MBIM indicates the partial interaction energy  $E_{a,0}(\hat{g})$  for the intra-clique shift  $a \in \mathbf{W}$ , the diametrically opposite shifts  $(x, y)$  and  $(-x, -y)$  representing the same clique family. In these examples the set  $\mathbf{W}$  contains the relative inter-pixel  $x$ - and  $y$ -shifts in the range  $[-40, 40]$  specifying 3280 clique families. In line with the chosen greyscale coding, the larger the energy value, the darker the dot.

The interaction structure  $\mathbf{A} \subset \mathbf{W}$  and potentials  $\mathbf{V}$  estimated for the model in Eq. (1) allow for simulating a desired texture from an arbitrary initial sample using pixel-wise stochastic relaxation combined with refinement of the potentials by stochastic approximation. The simulation brings close together the relative frequency distributions of signal co-occurrences for the characteristic clique families  $\{\mathbf{C}_a : a \in \mathbf{A}\}$  in the training and simulated textures [4, 5, 11].

Many stochastic image textures from [1] and [8] such as sand, pressed cork, grass lawn, wood grain, flowers, or metals are accurately simulated using quite small analytically estimated neighbourhoods of size  $|\mathbf{A}| \leq 10 \dots 20$ . The realistic simulation is obtained also for some regular mosaics but at the expense of much larger analytically estimated neighbourhoods [5]. Empirical learning [11] reduces the neighbourhoods, but involves too large amounts of computations per pixel. In any case some visually important fine details such as, for instance, small inclined strokes of the netting D34 in Figure 1 or short horizontal borders of the brick wall D95 in Figure 2 are not caught even with very large empirically or analytically found neighbourhoods. Also, because stochastic relaxation starts from an arbitrary image (usually, from a ‘‘salt-and-pepper’’ random noise), the overall periodicity of a large-size mosaic cannot be completely restored even if the local fine details are accurately reproduced.

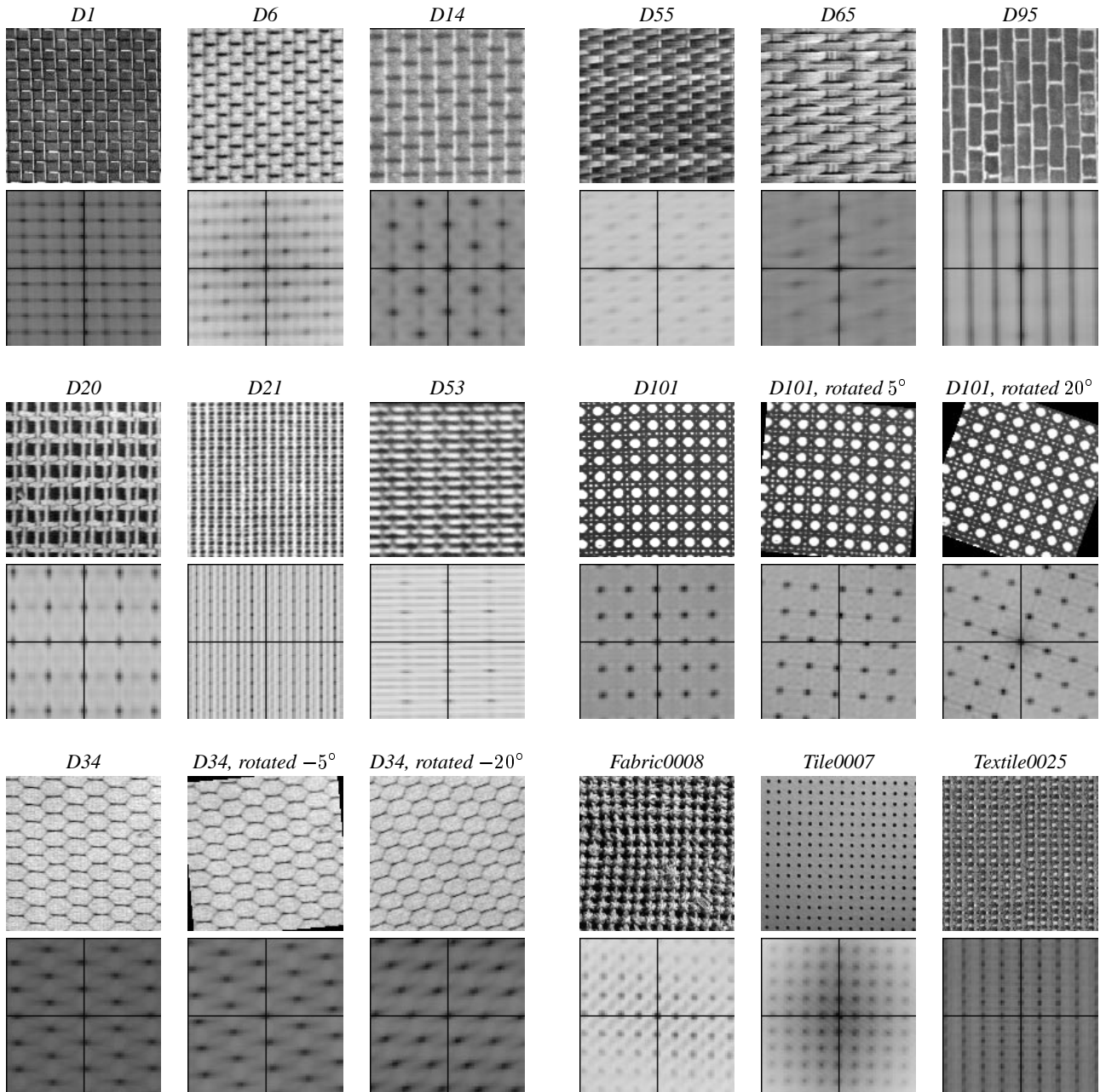


Figure 1: *Training samples and their MBIMs.*

Figure 2: *Training samples and their MBIMs.*

### 3 Estimation of texel parameters

To simulate (if possible) more realistic samples of complex natural textures by probabilistic modelling, large pixel neighbourhoods [5] or joint interactions of multiple pixels [9] should be taken into account. But it is computationally unfeasible to obtain a large-size texture by stochastic relaxation or multivariate optimisation that approximate training neighbourhoods with simulated signals. At the same

time a practicable alternative for some regular mosaics is to simulate a large-size prototype by tiling, that is, by spatial replication of the texel. Generally, each tile may have specific deviations from the texel.

As is easy to see in Figures 1 and 2, the MBIMs for the Gibbs model of Eq. (1) describe to a large extent the repetitive pattern of each texture. In particular, replicate spatial clusters of the larger interaction energies relate directly to translationally similar replicate parts of the periodic mo-

saics. The relative positions of and pitches between the clusters reflect the overall rectangular or hexagonal spatial arrangement, orientation, and shapes of the parts. In the above examples each such part acts as a single texel although the choice is not unique because the same MBIM defines different but equivalent tilings with different biases with respect to the lattice. The size of the texel is bounded only below that stems from the assumed translational similarity of all its replicas forming the training or simulated texture. In the general case it is difficult to formally relate the repetitive pattern of the MBIM to a minimum-size texel because some of the energy clusters may arise from repetitive fine details of the texel itself or from the secondary interactions between the distant similar parts. The shape and scale of the tiles representing a single texel as well as their photometric characteristics may also vary for different training samples and even within the same sample of the texture (see, for instance, the samples D55 or Fabrics0008 in Figure 2).

For simplicity, our consideration is restricted to only a rectangular texel with an arbitrary but fixed orientation and size. Each texture in Figures 1 and 2 is more or less accurately described as a tiling with translation invariant rectangular tiles representing such texel. For instance, the overall patterns of clearly defined energy clusters for the original and rotated by  $\pm 5^\circ$  and  $\pm 20^\circ$  textures D34 and D101 are oriented with respect to the Cartesian axes of the inter-pixel  $x$ - and  $y$ -shifts in the MBIM as do the corresponding tilings with respect to the  $x$ - and  $y$ - Cartesian axes of the training sample. Thus the orientation and size of the rectangular texel can be in principle derived from the MBIM.

The central cluster of the most energetic close-range interactions in the MBIMs relates mainly to a uniform background of the image but a repetitive pattern of the peripheral clusters (if it exists) is produced by the characteristic long-range similarities between the pixel pairs. Therefore it is felt that a single rectangular texel can be selected by circumscribing the clearly defined peripheral energy clusters placed around of and closest to the central cluster.

Figure 3 demonstrates the estimated partitions of the training samples where each rectangular tile represents the texel. These experiments are based on a simplified heuristic estimation scheme:

- (i) Form the MBIM  $\mathbf{E}(\hat{g})$  for a given training sample  $\hat{g}$  by computing the partial energies of Eq. (2).
- (ii) Select the clearly defined spatial clusters of the energies by thresholding the MBIM with an empirical threshold:

$$E^* = \bar{E} + c \cdot \sigma_E \quad (3)$$

where  $c$  is a heuristically chosen factor and  $\bar{E}$  and  $\sigma_E$  denote the mean value and standard deviation of the partial energies  $\mathbf{E}(\hat{g})$ , respectively.

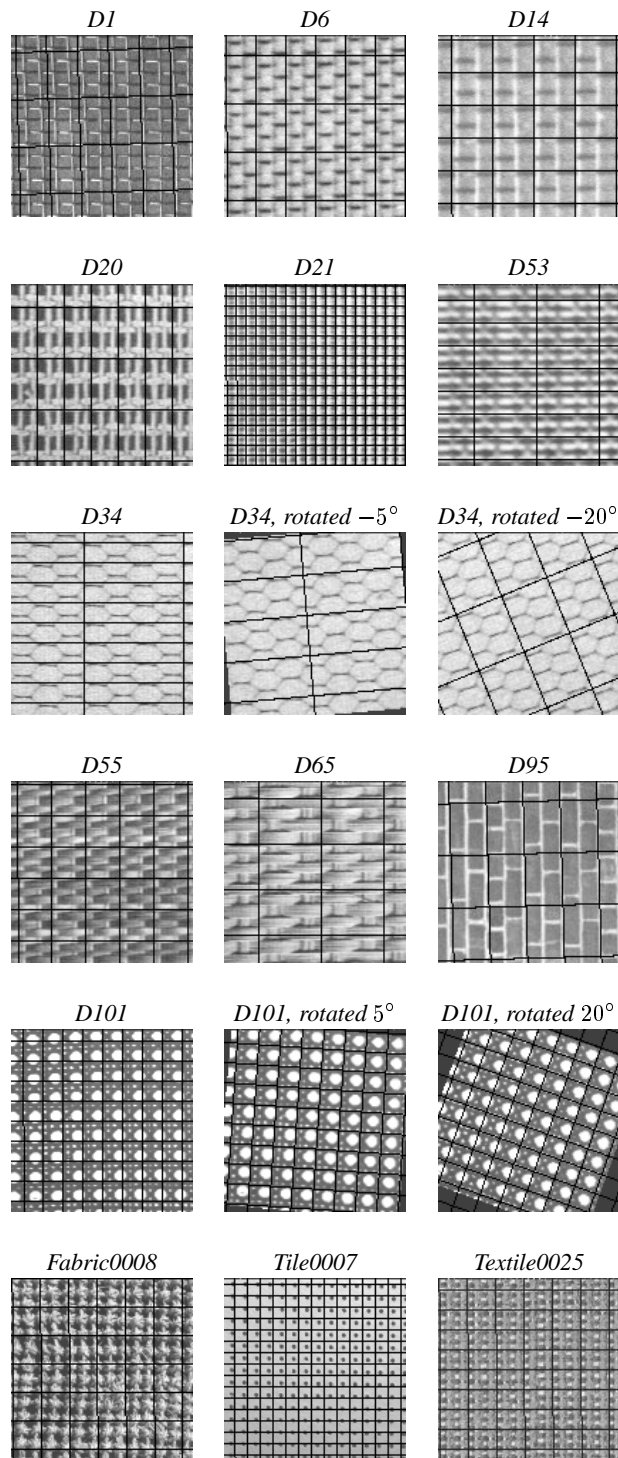


Figure 3: *Estimated partitions of the training samples.*

- (iii) If there are no peripheral clusters in addition to the central cluster around the origin  $a = (0, 0)$ , then the texture has no regular structure to be described by the

texel.

- (iv) Otherwise specify each peripheral cluster by its maximum energy and the inter-pixel shift for the clique family yielding this maximum and select two top-rank clusters (with the largest and the second largest energy) providing that the first cluster does not occlude another one from the origin of the MBIM.
- (v) Using the selected two clusters, find the texel orientation by choosing the smallest angular inter-pixel shift with respect to the  $x$ -axis of the MBIM and determine the texel size by projecting both inter-pixel shifts to the found Cartesian axes of the texel.

Table 1 gives parameters of the texels and tilings in Figure 3. Changes of the thresholding factor  $c$  of Eq. (3) in the range  $1 \leq c \leq 3$  yield quite similar results for all the textures used in the experiments.

Table 1: *Texel parameters estimated by detecting the first and second top-rank energy clusters in the MBIMs with the factor  $c = 2.5$  in Eq. (3).*

Texture	Estimated texel	
	Size, pixels ( $x \times y$ )	Orientation angle
D1	21.50 $\times$ 33.02	-1°.14
D6	21.00 $\times$ 34.00	0°.00
D14	29.00 $\times$ 23.00	0°.00
D20	19.00 $\times$ 36.00	0°.00
D21	7.00 $\times$ 7.00	0°.00
D34	70.00 $\times$ 14.00	0°.00
rot. -5°	70.26 $\times$ 28.24	-4°.90
rot. -20°	34.47 $\times$ 42.15	-22°.31
D53	44.00 $\times$ 16.00	0°.00
D55	24.00 $\times$ 22.00	0°.00
D65	44.00 $\times$ 32.00	0°.00
D65	44.00 $\times$ 32.00	0°.00
D95	25.96 $\times$ 36.76	-1°.64
D101	14.00 $\times$ 14.00	0°.00
rot. 5°	15.10 $\times$ 14.04	3°.81
rot. 20°	15.20 $\times$ 13.92	19°.65
Fabric0008	20.00 $\times$ 20.00	0°.00
Tile0007	9.00 $\times$ 8.00	0°.00
Textile0025	20.00 $\times$ 14.00	0°.00

The most important problem is to find the proper orientation of the texel. MBIMs with rectangular and hexagonal patterns of the clearly defined clusters yield sufficiently accurate and stable orientation estimates at Step (v). Moreover, the estimated orientation can be further refined by taking account of linear chains of the repetitive clusters, e.g. by finding the least scattered projections of the chains onto the

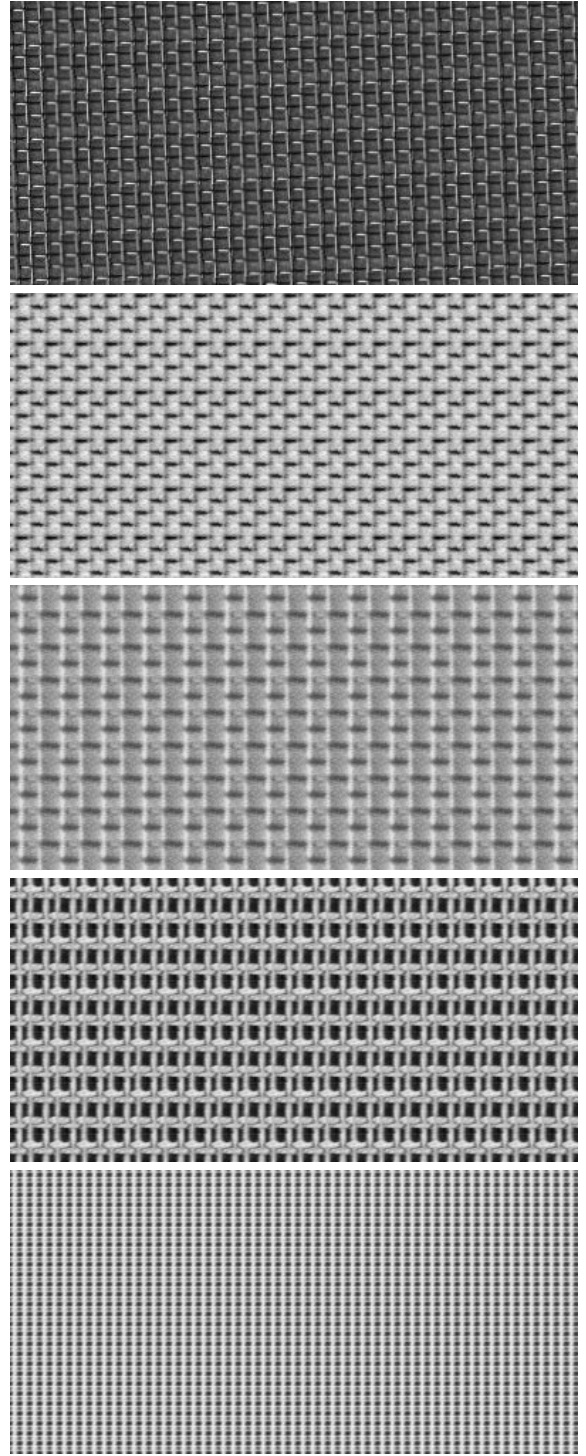


Figure 4: *Prototypes D1, D6, D14, D20, and D21 simulated by replicating the approximate texel.*

coordinate axes). But the refined estimates are less stable for the MBIMs with the hexagonal structures such as for the textures D34 or D65. In the general case much more detailed

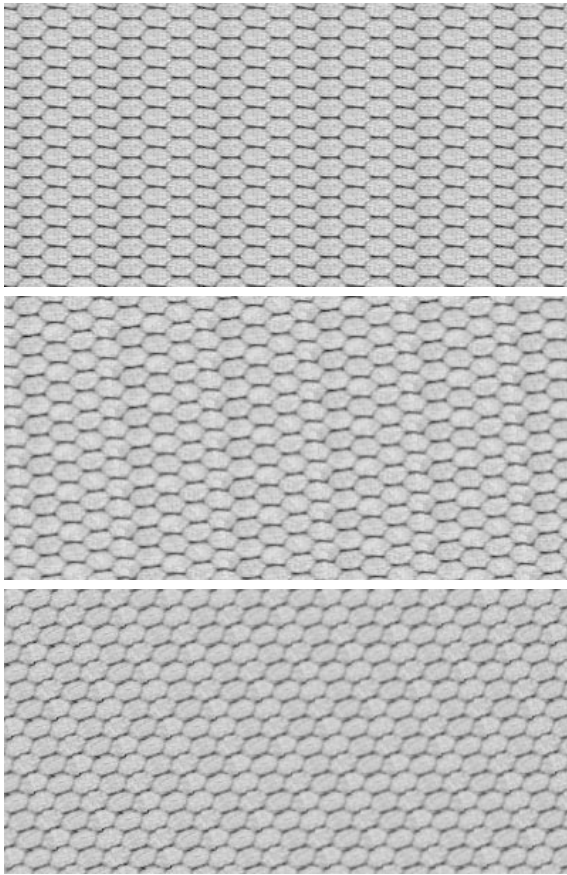


Figure 5: *Prototypes D34 (initial and rotated  $-5^\circ$  and  $-20^\circ$ ) simulated by replicating the approximate texel.*

processing of the MBIMs should be conducted for finding adequate shapes, sizes, and orientations of the texels. The above scheme is used to only show that it is possible in principle to formally define the texels by processing the MBIMs having specific spatial periodicity of the energy clusters.

Examples of the simulated prototypes of the size  $200 \times 400$  pixels are shown in Figures 4 – 8. Each prototype is obtained by replicating a single tile arbitrary chosen in the training sample in order to act as an approximate texel. Of course, such a straightforward simulation has obvious drawbacks in that the singularities of the chosen tile are replicated verbatim. The individual tiles cut out from the training sample may have deterministic or random distortions comparing to the desired texel. But all the tiles are explicitly specified by the estimated partition of the training sample so that they can be jointly processed as to exclude relative distortions and produce an ideal texel with no singularities. Also, to avoid the verbatim copies, the texel-based “rubber stretching” of the training sample can be done using bilinear or spline spatial interpolation of the intermediate replicas of the tiles.

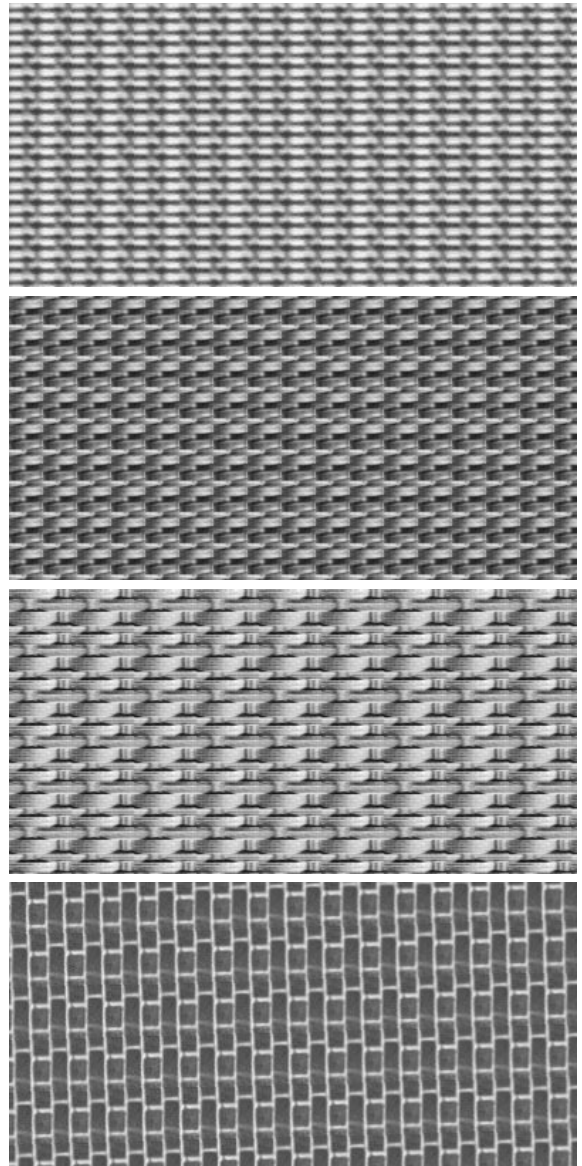


Figure 6: *Prototypes D53, D55, D65, and D95 simulated by replicating the approximate texel.*

## 4 Conclusions

The described scheme explicitly partitions the training sample onto a set of similar tiles representing the same rectangular texel. The orientation and size of the texel are deduced from the geometry of most characteristic pairwise pixel interactions in the training sample, that is, by analysing the spatial distribution of the partial interaction energies in the model-based interaction map.

Each tile can be used as a provisional texel but in principle the texel can be obtained by matching and joint processing of all the tiles so that their spatial compatibility is en-

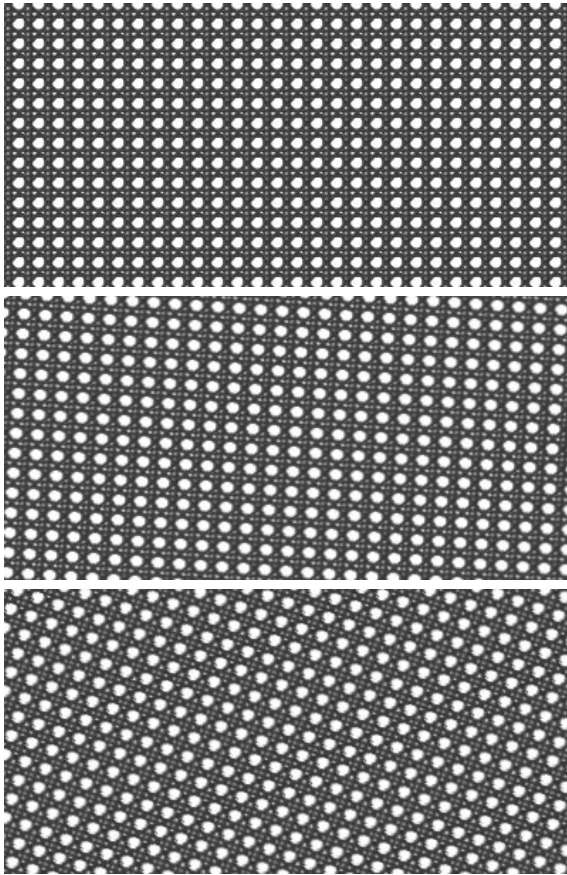


Figure 7: Prototypes D101 (initial and rotated  $5^\circ$  and  $20^\circ$ ) simulated by replicating the approximate texel.

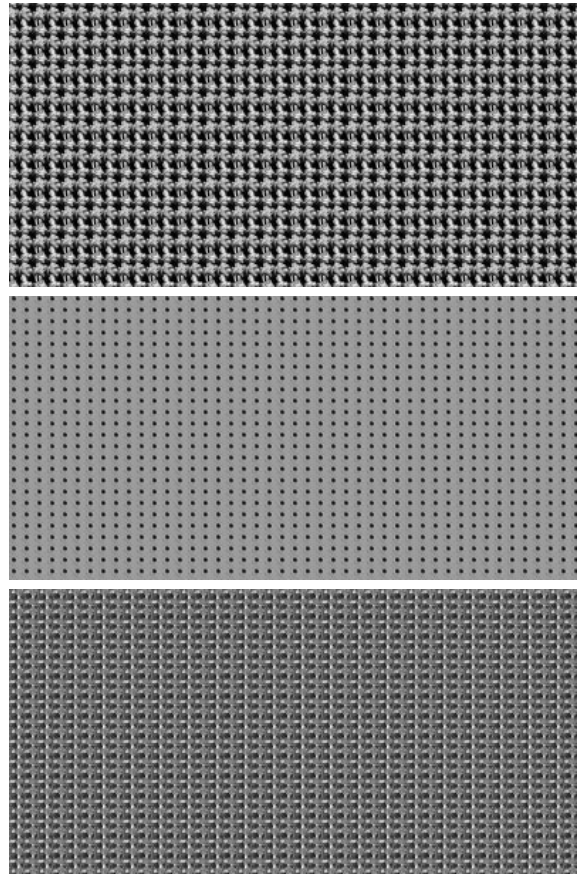


Figure 8: Prototypes Fabric0008, Tile0007, and Textile0025 simulated by replicating the approximate texel.

hanced and random geometric and photometric distortions are reduced. Replication of the texel forms an idealised prototype of the texture, and more realistic samples can be obtained by additional spatially consistent deterministic and random transformations of each tile in the prototype.

The proposed texel-based description is not adequate for all irregular (stochastic) textures that involve a large number of spatially discontinuous texels and complicated stochastic rules of their spatial arrangement. Their MBIMs contain usually only a central energy cluster with no peripheral repetitive ones. Such deterministic interaction structures are better described in terms of translation invariant conditional probability distributions of signal co-occurrences in the characteristic pixel neighbourhoods. But the texel-based description seems to be quite practicable for some translation invariant regular mosaics.

At present most advanced texture simulation is obtained by using the training sample as a collection of most characteristic pixel neighbourhoods. By this strategy the training neighbourhoods are implicitly or explicitly approximated by the like neighbourhoods of the simulated image. The ap-

proximation is based either on specific integral features of the signals in the neighbourhood or directly on these signals. The proposed texel-based description provides the texel as the explicit most characteristic pixel neighbourhood to be estimated from the training sample and approximated in the simulated images. Because the estimation is computationally simple, the use of the texels notably accelerates the simulation of the large-size samples of regular mosaics.

## References

- [1] Brodatz, P., *Textures: A Photographic Album for Artists and Designers*, Dover Publications, New York, 1966.
- [2] J. S. De Bonet, "Multiresolution Sampling Procedure for Analysis and Synthesis of Texture Images", in: *Proc. ACM Conf. Computer Graphics SIGGRAPH'97*, 1997, pp.361–368.

- [3] A. A. Efros and T. K. Leung, "Texture Synthesis by Non-Parametric Sampling", in: *Proc. IEEE Int. Conf. Computer Vision ICCV'99, Greece, Corfu, Sept. 1999*, vol. 2, 1999, pp.1033–1038.
- [4] Gimel'farb, G. L., *Image Textures and Gibbs Random Fields*. Kluwer Academic, Dordrecht, 1999.
- [5] G. Gimel'farb, "Characteristic Interaction Structures in Gibbs Texture Modeling", in: Blanc-Talon, J. and D. C. Popescu (Eds.), *Imaging and Vision Systems: Theory, Assessment and Applications*, Nova Science, Huntington (N.Y.), 2001, pp.71–90.
- [6] Haralick, R. M. and L. G. Shapiro, *Computer and Robot Vision*, vol. 2, Addison-Wesley, Reading, 1993.
- [7] Liang, L., C. Liu, Y. Xu, B. Guo, and H. Y. Shum, *Real-Time Texture Synthesis by Patch-Based Sampling*. MSR-TR-2001-40. Microsoft Research, 2001, 21 p.
- [8] Pickard, R., S. Graszcyk, S. Mann, J. Wachman, L. Pickard, and L. Campbell, *VisTex Database*, MIT Media Lab., Cambridge (Mass.), 1995.
- [9] R. Paget and I. D. Longstaff, "Texture Synthesis via a Noncausal Nonparametric Multiscale Markov Random Field", *IEEE Transactions on Image Processing*, vol.7(6), 1998, pp.925–931.
- [10] J. Portilla and E. P. Simoncelli, "A Parametric Texture Model Based on Joint Statistics of Complex Wavelet Coefficients", *Int. Journal on Computer Vision*, **40**(1), 2000, pp.49–71.
- [11] A. Zalesny and L. Van Gool, "A Compact Model for Viewpoint Dependent Texture Synthesis", in: Pollefeys, M., L. Van Gool, A. Zisserman, and A. Fitzgibbon (Eds.), *3D Structure from Images (Lecture Notes in Computer Science 2018)*, Springer, Berlin, 2001, pp.124–143.